

Bachelor's Thesis

Liquid water content from airborne radar and radiometer measurements

Imke Schirmacher

Imke.Schirmacher@studium.uni-hamburg.de

Course of studies: B.Sc. Meteorology

Matriculation number: 6916094

Semester: 6

Primary supervisor: Dr. Heike Konow

Secondary supervisor: Prof. Dr. Felix Ament

Submission deadline: November 18, 2019

Liquid water content from airborne radar and radiometer measurements

Abstract

During the NARVAL South campaign in December 2013 and NARVAL2 campaign in August 2016 over the North Atlantic near Barbados, measurements of the liquid water path and equivalent radar reflectivity were taken by the HALO Microwave Package including a microwave radiometer and a cloud radar. The aim of this study is to calculate the liquid water content based on these measurements. In a second step, the liquid water content is correlated with typical cloud characteristics like type of cloud, cloud height and cloud depth. In addition, the difference between liquid water content of precipitating, non-precipitating clouds and rain is investigated. The analysis mainly concentrates on shallow cumulus clouds formed below the trade wind inversion.

The result of this study is that below the trade wind inversion the average of the cloud liquid water content is around 0.2 g m^{-3} , aloft it is less with 0.1 g m^{-3} . Deep convective clouds are not capped at the inversion, thus the humidity is distributed over the whole troposphere which leads to a constant distribution of moderate liquid water content.

The liquid water content of shallow cumulus clouds also depends on cloud depth. For clouds with a depth up to 500 m it is increasing linearly with depth. The increase is case dependent reaching values up to 0.25 g m^{-3} . 0.5–1.7 km deep clouds have a constant liquid water content of around 0.15 g m^{-3} and deeper clouds of 0.30 g m^{-3} , respectively. This means that dry intrusion is not that relevant for clouds deeper than 1.7 km compared to clouds with a depth of 0.5–1.7 km.

During wet season the liquid water content of non-precipitating shallow cumulus clouds is greater than during dry season. The average of precipitating shallow cumulus clouds is relatively constant throughout the year, with values of about 0.19 g m^{-3} . This leads to the result that clouds with high LWC are non-precipitating during wet season, but precipitating during dry season. Rain has always a lower liquid water content than shallow cumulus clouds.

Contents

List of Abbreviations	III
1 Introduction	1
2 Data	4
2.1 NARVAL campaigns	4
2.2 HAMP	5
2.3 Preprocessing of available data	5
3 Calculations	7
3.1 Liquid water content	7
3.2 Lifting condensation level	8
4 Cloud, LWP and LWC distribution	9
4.1 Results	9
4.2 Discussion	13
5 Dependency of LWC on altitude	16
5.1 Results	16
5.2 Discussion	18
6 LWC dependency on cloud depth	21
6.1 Results	21
6.2 Discussion	22
7 Difference in LWC of rain, precipitating and non-precipitating clouds	25
7.1 Results	25
7.2 Discussion	26
8 Conclusions and outlook	29
List of Figures	33
References	34

List of Abbreviations

CCN cloud condensation nuclei

CR cloud radar

HALO High Altitude Long range

HAMP HALO Microwave Package

ITCZ Inter-Tropical Convergence Zone

LCL lifting condensation level

LWC liquid water content

LWP liquid water path

MWR microwave radiometer

NARVAL Next-generation Aircraft Remote sensing for Validation studies

RH relative humidity

1 Introduction

Clouds determine the water and energy cycles as well as the radiation budget on earth (Oh et al., 2018). Thus, clouds and precipitation are very important for climate and water is the most important atmospheric component (Stevens and Bony, 2013a). The forming of clouds and micro-physical processes inside clouds are very complex (Jacob et al., 2019a). Hence, clouds are poorly resolved in numerical weather models which leads to wrong forecasts in precipitation and climate predictions (Oh et al., 2018; Löhnert et al., 2001; Stevens and Bony, 2013b). The modelling of marine clouds, as trade wind cumulus clouds, is even more difficult because they are too shallow to be resolved by remote satellites correctly (Jacob et al., 2019a).

Barbados, which is the measurement site for this study, is a suitable place for observing trade wind clouds. The clouds near Barbados are influenced by the global circulation (see Fig. 1). The global circulation is driven by an ascend of warm air at the equator. Radiative warming and additional release of latent heat during condensation of water inside the rising air parcel reduce the density of the parcel and lift it. The region of ascending air is called Inter-Tropical Convergence Zone (ITCZ). At the top of the troposphere, up to 18 km, the air moves polewards and descends at the horse latitudes at 30° . In between these two areas are the low altitude trade winds, where the air is moving back to the equator. The circulation cell is called Hadley cell. Due to the spherical shape of the globe, the moving air parcels aloft get compressed by moving polewards. Thus, they have to flow downwards. The descending air masses are heated dry adiabatically whereas the ascending air parcels from the trade winds, warmed by radiation, cool saturated adiabatically. The equatorial air masses are still warmer than the trade wind air parcels. Hence, the trade wind inversion at 2–3 km altitude evolves (Riehl, 1979).

Barbados, located at 13°N , is influenced by the trade wind during dry season. During wet season the ITCZ is moving northwards by a few degrees, influencing the Barbados region (Medeiros and Nuijens, 2016). In the trade wind regions are no deep clouds compared to the convective clouds inside the ITCZ (see Fig. 1). This is because the trade wind inversion prevents air from ascending, which leads to a formation of trade wind clouds at around 1 km height, classified as shallow cumulus (Riehl, 1979).

Cloud droplets of these warm clouds form by heterogeneous nucleation on cloud condensation nuclei (CCN). For this process, an air parcel with dry aerosols inside is lifted first. Meanwhile, the RH is increasing. If the RH is just below 100%, water vapour will condensate on the aerosols and fog will be produced. The sizes of the particles increase, depending on air moisture. In the next step, the droplets get activated. This process is predetermined for each droplet by its Köhler-curve. The activated droplets grow without any restrain as long as RH is greater than 100%. They absorb all moisture greater than 100%, which leads to no new activations of droplets. Then, the cloud droplets are growing through condensation. The growth is limited by the speed of diffusion. Thus,

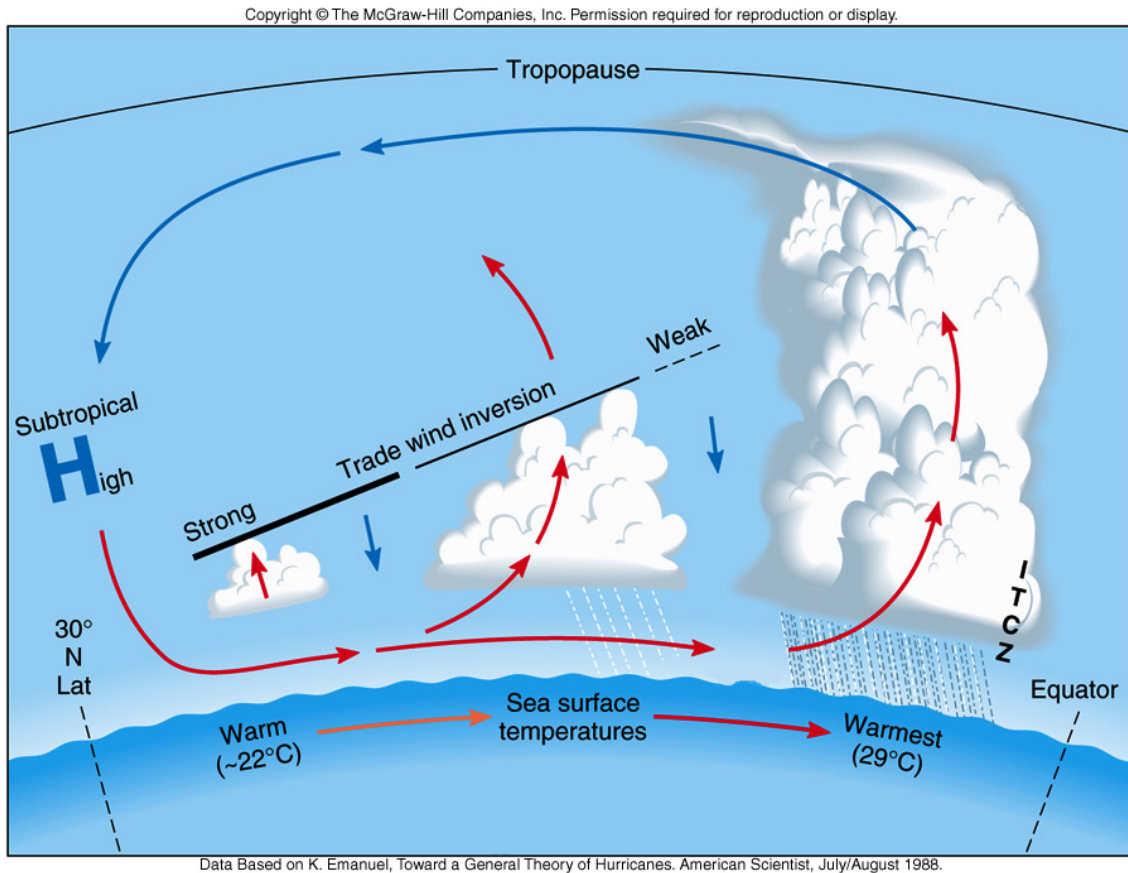


Figure 1: Conceptual model of the vertical profile of the Hadley cell across the tropical North Atlantic (by Tes blendspace (2019), modified by Imke Schirmacher).

large droplets grow slower than small ones. In the end, all cloud droplets from continental clouds have the same radius of around $10\ \mu\text{m}$. This kind of growth is valid for non-precipitating, warm cumulus clouds a few hundred meters above the cloud base. Thus, it is the mechanism for the formation of cloud droplets in the analysed cases. Nevertheless, in marine air there are fewer CCN than in continental air while the LWC is the same. This leads to a greater droplet size for marine than for continental clouds. Hence, marine cloud droplets have a radius of about $20\ \mu\text{m}$. Additionally, sea spray brings salt particles into the lower troposphere, which are also large aerosols up to $10\ \mu\text{m}$ (Levin and Cotton, 2008) and act like giant CCN.

Raindrops, however, have a radius of $1\ \text{mm}$, about two orders of magnitude bigger. Hence, a different process is necessary to form raindrops, which happens by collisions between cloud droplets. Large droplets fall faster than small droplets, thus they collect smaller droplets and form one big droplet. The stochastic collection describes the effect that large droplets are more likely to collide with other droplets. Hence, large droplets grow faster and the differences in size increase. The larger droplets of $20\ \mu\text{m}$ in radius over sea and sea spray form larger rain drops than over land. As a result, maritime clouds rain earlier than continental clouds (Wallace and Hobbs, 2006).

The parameter describing clouds in weather models is the liquid water content (LWC).

It describes the amount of water in a unit bulk of dry air. Because it is a lot harder to observe LWC, most researchers concentrate on measuring the liquid water path (LWP), which describes the total mass of liquid water in an atmospheric column above an unit area (Jacob et al., 2019a). The LWP is equivalent to the vertically integrated LWC over the atmospheric column.

In this study, the LWC of marine clouds over the North Atlantic is calculated from LWP measurements. The data were gathered by the HALO Microwave Package (HAMP), including a microwave radiometer (MWR), a cloud radar (CR) and dropsondes during the Next-generation Aircraft Remote-sensing for VALidation (NARVAL) South campaign in December 2013 and NARVAL2 campaign in August 2016 over the North Atlantic near Barbados (Mech et al., 2014). The LWC is analysed for this data set for the first time (Jacob et al., 2019a). The main aspect of this study is the investigation of the LWC distribution in shallow cumulus clouds. This type of cloud is of particular interest because of its large climatic effect. However, weather models are only able to poorly resolve them. This study can help to better represent shallow cumulus clouds in weather models in future. Additionally, convective clouds are analysed, as they are another important cloud type for the Barbados region in wet season.

First of all, the NARVAL campaigns, during which the measurements were taken, are presented (Sec. 2.1). Next, the measurement instruments called HAMP are explained and specified (Sec. 2.2). In Sec. 2.3 the preprocessing of the data, which is done for this thesis, is explained, before the LWC is calculated for this processed data set in Sec. 3.1. The results of the analysis are presented in the following sections, starting with the distribution of the clouds, the measured LWP and calculated LWC for three selected flights in Sec. 4. Then, the evolution of LWC with height in the atmosphere (Sec. 5) and with cloud depth (Sec. 6) is analysed. The last aspect is looking at the difference of LWC inside shallow cumulus clouds and rain (Sec. 7). An additional separation into precipitating and non-precipitating clouds is done.

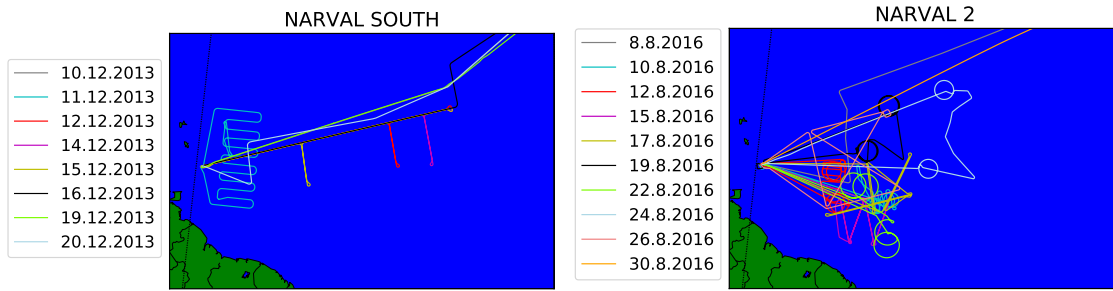


Figure 2: Flight pattern of all flights during NARVAL South (left) and NARVAL2 (right). Each campaign day is indicated by its own color. The map section is near Barbados.

2 Data

The following section is about the observed data. First, the aim and structure of the NARVAL campaigns are explained (Sec. 2.1). During this campaigns the data for this study were measured by a set of instruments, which is called HAMP (Sec. 2.2). Also the preprocessing of the used data by Konow et al. (2018a), Konow et al. (2018b), Jacob et al. (2019b) and Jacob et al. (2019c) is mentioned in Sec. 2.3.

2.1 NARVAL campaigns

The analysed data were measured during the Next-generation Aircraft Remote-sensing for VALidation (NARVAL) campaigns. The aim of these field studies is to improve the understanding of clouds, their effect on the distribution of water in the atmosphere, as well as the interaction between clouds and their environment (Bony et al., 2017). Also models resolving cloud-scale circulations are evaluated (Miyamoto et al., 2013; Klocke et al., 2017). During four missions HALO was flying as a remote sensing cloud observatory with active and passive sensors on board. The MWR and the CR made up the HAMP, which will be presented in detail in the following section (Mech et al., 2014).

Until the NARVAL campaigns, airborne laboratories dominantly made in-situ measurements, while Satellites and ground based stations measured remotely with spatial limitation. During NARVAL the spatial resolution of an aircraft and the high temporal resolution of remote sensing instruments were used at once for the first time (Stevens et al., 2019). Also, dropsondes were used for in-situ measurements.

NARVAL consists of four aircraft campaigns altogether. These aircraft campaigns are the NARVAL1 expedition during December 2013 over the winter trades of the tropical North Atlantic (NARVAL South, Fig. 2a) and during January 2014 over the extra tropical North Atlantic (NARVAL North). The NARVAL2 mission during August 2016 was, like during NARVAL South, over the tropical North Atlantic and the Atlantic ITCZ (Fig. 2b).

The North Atlantic Waveguide Downstream Experiment (NAWDEX) was over the extra tropical North Atlantic (Stevens et al., 2019). In this study, the measurements over the tropical North Atlantic from NARVAL South and NARVAL2 are analysed.

2.2 HAMP

HAMP is a set of instruments to investigate the radiant energy over the electromagnetic spectrum. It consists of a Ka-band CR at 35.5 GHz and three MWR with 26 frequencies between 22.24 GHz and 183.31 ± 12.5 GHz. The MWR with an integration time of 1 s and a resolution in along-flight direction of 1.4–0.9 km and in across-flight direction of 1.1–0.6 km for a flying altitude of 13.0 km restricts the spatial resolution of HAMP. However, the spatial resolution of HAMP of around 1 km is better than the 50 km resolution of passive satellite observations like the SSM/I (Bremen et al., 2002).

Instruments operating in the microwave spectrum are able to observe clouds and precipitation because liquid water is semitransparent in their spectral region. For e.g. the active microwave CR resolves profiles of backscattered signals by hydrometeors. The signal of this radar gets less reduced due to condensate than radars operating with different microwave frequencies. It is also able to observe strong gradients in reflectivity because it is monostatic and pulsed. The vertical resolution of the radar is 30 m and the temporal resolution is 1 s (Mech et al., 2014). However, the CR is less accurate resolving clouds with a small number of hydrometeors than the MWR.

2.3 Preprocessing of available data

The used data were preprocessed by Konow et al. (2018a), Konow et al. (2018b), Jacob et al. (2019b) and Jacob et al. (2019c) before additional study-specific processing is done in Sec. 3.1. This study is primarily based on the evaluation of the equivalent radar reflectivity factor Z in dBZ (represented by dBZ in Eq. (1)) of the HAMP CR data. It is defined as

$$dBZ = 10 \cdot \log_{10} Z \quad (1)$$

with Z being the reflectivity factor in $\text{mm}^6 \text{m}^{-3}$. More and bigger raindrops result in higher reflectivities at the CR wavelength, which produce higher Z . A Z of 40 dBZ indicates moderate rain, whereas negative values are produced by a water amount less than light drizzle or insects (Fabry, 2015).

The Z data for this study are taken from the CR files from Konow et al. (2018a) and Konow et al. (2018b), where Z is given as a profile over the whole flight with gates of 30 m height, starting at 0 m above the surface. The provided radar data quality flag,

which discards unreliable data from the analysis that are e.g. affected by ground cluttering or radar calibration maneuvers, is applied to Z for this study. A rough surface does not only reflect the electromagnetic pulses of the radar specularly, but also scatters the signal diffusely and backward. The diffuse backscatter towards the radar is the ground clutter and will be called sea clutter, if it is produced by waves (Watts et al., 2016). Trapping of the beams by the lowest waves, instead of refracting upward, and also evaporation increases the height of clutter (Karimian et al., 2011). Thus, some reflectivity Z in the first layers above the surface is not from clouds.

With help of the MWR, the CR and the lidar WALES, time series of LWP with offset correction and an appendant status flag are retrieved by Jacob et al. (2019b) and Jacob et al. (2019c). These LWP values are corrected with the aid of the status flag for this study. Thereby, events with LWP values above 1 kg/m^2 are not analysed because the measurements are considered uncertain. Frozen precipitation is removed as well because the measurements are imprecise for ice. In addition to these measurements, a cloud mask filtering the radar measurements for clouds and numbering each cloud by Konow (2019) is used in Sec. 6 and 7. The temperature and relative humidity measurements by the sondes are taken from the sonde file from Konow et al. (2018a) and Konow et al. (2018b). They are used for the calculation of the lifting condensation level (LCL) (Sec. 3.2).

3 Calculations

So far, only the LWP, but not the LWC, was analysed from the NARVAL campaigns data set (Jacob et al., 2019a). Thus, it is calculated in Sec. 3.1. Also, a separation of the observed CR signals and calculated LWC values into values caused by rain or clouds is necessary in this study. Hence, a second calculation was done in advance, which is explained in Sec. 3.2. Thereby, the height of the LCL is derived.

3.1 Liquid water content

For this study, the LWC is calculated for eight flights, four from NARVAL2 on August 12, August 15, August 19 and August 22, 2016 and four from NARVAL South on December 11, December 12, December 14 and December 15, 2013. August 10 and August 17, 2016 are left out due to failing of the MWR. Also, the four arrival and departure flights are not analysed.

The weather and cloud cover during these days are different, however, have no seasonal correlation. They do not represent the wet or dry season. On August 12 and August 19, 2016, a divergence existed. On December 12, December 14 and December 15, 2013, HALO was flying above the trade winds. Very different conditions are found on August 22, 2016, where the measurements were taken in the inner ITCZ. On August 15, 2016, the aircraft was crossing the ITCZ and the flight on December 11, 2013 was in adjacent regions of the ITCZ (Stevens et al., 2019).

As a first additional preprocessing step, radar reflectivities with a height of only one gate are removed, because there the radar signal is assumed to be reflected by insects or other small objects in the atmosphere, but not by a cloud. Clouds normally have a larger depth than 30 m, thus covering at least two gates. After applying all flags mentioned in Sec. 2.2, values from the lowest four levels above the surface are removed (0 up to 120 m). This is done as the radar flag proved not to be reliable for removing the ground cluttering. Sometimes the LWP is slightly negative. These values are set equal to zero, because of physical plausibility. The CR does not observe clouds with a low number of hydrometeors, whereas the MWR is more accurate and measures low LWP. Setting the LWP to zero will only lead to a positive bias of the LWC. However, no clouds are neglected by this process.

The LWC at any gate p , q_p , is calculated by

$$q_p = \frac{Q\sqrt{Z_p}}{\sum_{j=1}^{j=M} \sqrt{Z_j}\Delta h} \quad (2)$$

with Q being the LWP, Z_p and Z_j being the equivalent reflectivity factor in dBZ at gate p and j respectively, Δh being the gate length and M being the number of the highest gate inside the cloud (Frisch et al., 2000). For M , the highest gate of the flight is taken, because the gates above a cloud have no radar reflectivity, thus do not contribute to the sum. The vertical resolution Δh between two gates is 30 m in this study.

Clouds in the upper troposphere mostly consist of ice and only a bit of liquid water. Thus, much of the equivalent reflectivity factor of these clouds comes from cloud ice. For the sake of simplicity, in this study the LWC is defined as the water content including the water content from cloud ice.

3.2 Lifting condensation level

The CR only gives information about the amount of hydrometeors but does not distinguish between rain and clouds. To differentiate between a cloud and rain, the following calculation is used to get the height of the lifting condensation level z_{LCL} :

$$z_{LCL} \approx (20 + \frac{t}{5})(100 - RH) \quad (3)$$

with t being the dry-bulb surface temperature in degrees Celsius and RH being the relative humidity near the surface in percent. The LCL is the level at which an unsaturated, moist air parcel gets saturated regarding a surface of water after adiabatic lifting (Wallace and Hobbs, 2006). The LWP includes the rain water and cloud water path. Thus, the calculated LWC also includes both, the water content of rain and clouds. LWC values above the z_{LCL} are due to clouds and below due to rain. For this study temperature and relative humidity measurements from the sondes just above the surface are taken for t and RH for all eight flights. The gained height for one time step is interpolated for the other steps to get a height for every time even with only a few sondes.

4 Cloud, LWP and LWC distribution

After calculating the LWC, the LWC evolution with time is compared to the profile of the equivalent reflectivity factor observed by the CR and the LWP time series for all eight flights to investigate the connection between LWC and different cloud types. There seems to be a difference in LWC for deep convective clouds as well as for shallow cumuli in the lower or upper atmosphere. Additional LWC- and Z-frequency distributions and distributions of the cloud fraction and cloud bases with altitude are analysed. This gives an overview of the relevant meteorological parameters during the analysed days and says something about the meteorological conditions. E.g. different types of precipitation and clouds affect the histogram of Z and LWC in different ways. The eight flights in total can all be assigned to one of three categories. For each category, one representative flight is analysed further.

4.1 Results

To get an idea of the meteorological conditions on December 11, 2013, the profile of the equivalent reflectivity factor (Fig. 3, second row) is analysed, which is similar to the one on August 15, 2016 and December 14, 2013. The profile can be split into three sections. From the beginning of the flight until around 16:00 h, no clouds are observed by the CR. This is followed by a period with a shallow single cloud layer reaching an altitude of 3.1 km. At 19:10 h, a second cloud layer with its center at around 12 km height forms. It is mostly a separated, 4 km deep layer. It is the only cloud layer present for the first half of this period while the lower layer appears again in the second half. Nonetheless, the two cloud layers form one single cloud layer for around 5 minutes at 20:30 h. Looking at the lower cloud layer shows that roughly two types of clouds coexist. First, there are signals extending to the surface, other signals only reach 1.5–1.6 km. The signals ranging to the surface are precipitating clouds, the other signals are non-precipitating clouds.

To analyse the kind of clouds observed on December 11, 2013, the distribution of cloud fraction is investigated. The maximum cloud fraction is located at around 2 km with 7% of the overall measurement duration. In the upper level, the maximum cloud fraction is at around 12 km with 4% (Fig. not shown). Thus, there is a main shallow cloud layer in the lower troposphere and a second shallow cloud layer in the upper atmosphere. The cloud fraction of the altitudes in between are not relevant averaged over the whole measurement duration.

Z varies with the amount and size of the observed hydrometeors. Hence, the analysis of the Z-frequency distribution says something about the precipitation observed most frequently during the measurement duration. Z ranges from -50 to 40 dBZ with a maxi-

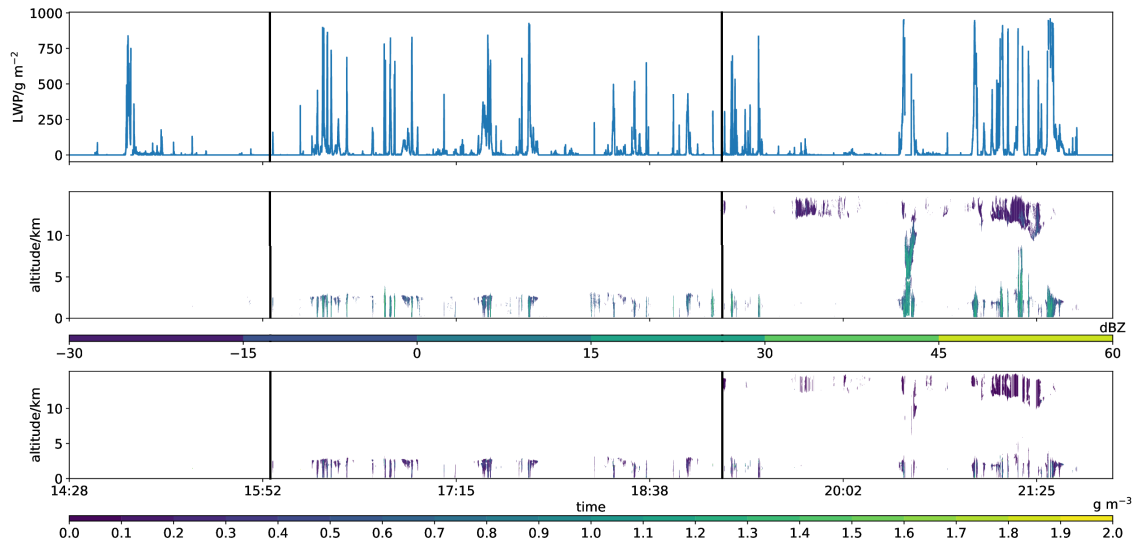


Figure 3: LWP time series in g m^{-2} (first row), profile of the equivalent reflectivity factor in dBZ with a separate color bar (second row) and calculated LWC distribution in g m^{-3} with a separate color bar (third row) for December 11, 2013. All x-axes cover the same time period. The black lines indicate the three sections, the profile can be split into.

imum of cases at -30 to -20 dBZ, indicating non-precipitating clouds (Fig. 4b). The range and distribution of the values are as expected. It is eye-catching that higher values of Z are distributed in the lower and connection layer, whereas the upper layer has lower Z values (Fig. 3 and Fig. 5). This is expected, as liquid water, which is mostly distributed in the lower layers, has higher Z than ice, which is the constituent of most hydrometeors in the upper layer. High values of Z mostly exist inside a bulk of signals, surrounded by lower values (see also Fig. 5, second panel). This result is discussed in the following section in detail.

To investigate the water content of the rain and clouds, it is worth having a look on the LWP values first. The LWP for areas with clouds only in the upper layer is significantly lower than that for areas with clouds only in the lower layer. This is because clouds in the upper layer mostly consist of ice, having a lower LWP than water, whereas clouds in the lower layer are mostly formed by liquid water. The LWP measurements show gaps mostly at points with high Z due to the LWP data flag by Jacob et al. (2019b) and Jacob et al. (2019c), which is described in Sec. 2.3 (Fig. 3, first panel). Peaks of LWP occur where Z signals extend to the surface. However, the correlation with large Z values does not seem to be that clear, because of the missing LWP data due to the data flag (also Fig. 5). To better distinguish between the water content of the different cloud layers, the LWC is investigated. The LWC values from the upper layer are smaller than from the lower one (Fig. 3, third panel). There seems to be a dependency of the LWC on the altitude in the atmosphere. This hypothesis is tested in Sec. 5. The LWC distribution follows the contours of Z , containing gaps where the LWP was set equal to zero due to the data

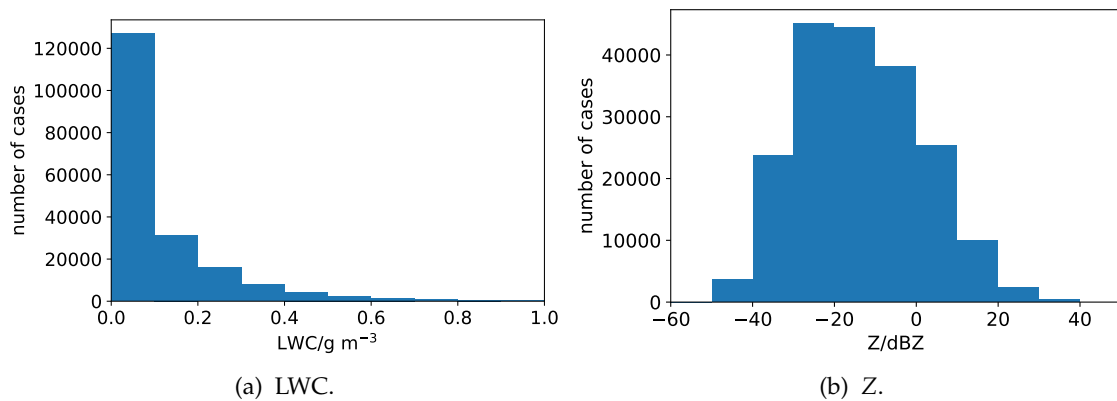


Figure 4: Histogram of (a) LWC in g m^{-3} and (b) Z in dBZ for December 11, 2013. Both y-axes show the number of cases.

flag (see also Fig. 5). As higher LWP values would look physically reasonable at these gaps, the gaps raise the question whether the limit of 1 kg m^{-2} for LWP as applied during the preprocessing by Jacob et al. (2019b) and Jacob et al. (2019c) was set too low and additional valuable information could be gained by reprocessing the data with a less restrictive limit. However, it has to be tested whether the used measurement techniques would be still accurate for the less restrictive limit. Most LWC data points, i.e. the LWC within a gate, range up to 1.0 g m^{-3} (Fig. 4a), as expected for non-precipitating clouds, with some outliers reaching up to 9.1 g m^{-3} . The number of LWC data points decreases hyperbolically with increasing LWC, because gates with high water content are less common. The amount of cases with a LWC between 0.1 and 0.2 g m^{-3} is only 24% of the number of cases from 0.0 (excluded) to 0.1 g m^{-3} (see Fig. 4a).

Compared to December 11, 2013 the clouds on December 12, 2013 show only one cloud layer at around $0\text{--}3 \text{ km}$ (Fig. 6). This cloud distribution is also given on August 12, August 19, 2016 and December 15, 2013. The distribution is similar to the first period of the one from December 11, 2013. Fig. 6 shows periods of no clouds with short isolated signals and phases with an accumulation of signals which are long lasting compared to the isolated ones. The Z distribution (Fig. not shown) is similar to the one on December 11, 2013, but it has a smaller spread from -30 to 40 dBZ . The very negative values up to -50 dBZ from December 11, 2013 are missing. Most cases are between -20 and -10 dBZ , thus 10 dBZ enhanced compared to December 11, 2013. A shift towards larger Z values is generated by a greater number of precipitating clouds. Again, there are two main altitudes of cloud bases, the surface and $1.1\text{--}1.2 \text{ km}$. Most clouds, with a cloud amount per altitude of 6% of the overall measurement duration, are at 1.8 km . Both altitudes are a few hundred meters lower than on December 11, 2013. In conclusion, the meteorological conditions changed. On December 12, 2013 only one layer of shallow cumulus is present in the lower atmosphere. The LWC (Fig. 6, third panel) has values up to 1.4 g m^{-3} , which is larger than the day before. The LWC distribution (Fig. not shown) also has a hyper-

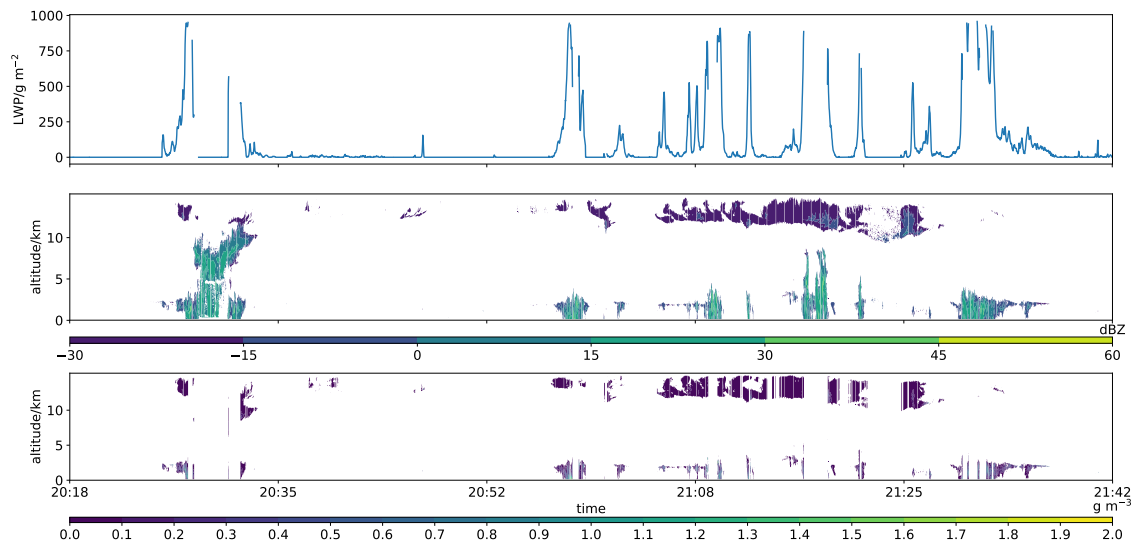


Figure 5: LWP time series in g m^{-2} (first row), profile of the equivalent reflectivity factor in dBZ with a separate color bar (second row) and calculated LWC distribution in g m^{-3} with a separate color bar (third row) for December 11, 2013. All x-axes cover the same time period. The profile is a close-up of Fig. 3, it is beginning at 20:18 h.

bolic decrease as on December 11, 2013. However, the difference between the amount of cases with a LWC from 0.1 until 0.2 g m^{-3} and between 0.0 (excluded) and 0.1 g m^{-3} is more than three times higher than on December 11, 2013. This indicates the observation of even more drier clouds compared to the amount of clouds with a high LWC on December 12, 2013 than on the day before.

The third observed cloud formation was on August 22, 2016 inside the ITCZ (Fig. 7). First of all, it is important to mention that the flying altitude there is only at around 10 km not 15 km like before. The maximum amount of clouds per altitude over the whole measurement duration is at 4.0 km, with slightly over 10% followed by somewhat less than 10% at about 9 km (Fig. not shown). Thus, one could roughly divide Z into two layers. The upper one is located at around 9 km and the center of the lower one at around 4 km. An additional, rarely visible layer is just below 2 km. This corresponds to the location of the cloud bases. A local maximum of cloud bases is at 1.3–1.5 km and a global maximum at 4.0–4.1 km. The upper level has the most cloud bases at 9.3–9.4 km. Much clouds are deeper than in Fig. 3 and Fig. 6. Most times, the signal bases are at the surface. These signals come from precipitation falling from clouds reaching a height of around 6 km. These clouds are no shallow cumuli, but deep convective clouds. Some are spreading continuously over the whole measurement height. Z is ranging from -70 dBZ to 30 dBZ with a maximum at -20 to -10 dBZ. This Z distribution (Fig. not shown) has the same course as before, but the widest spread. It has the lowest Z values compared to the other days. The maximum LWC is 0.6 g m^{-3} , only around half of the other LWC maxima. The number of cases with LWC from 0.1 to 0.2 g m^{-3} compared to to the number of cases

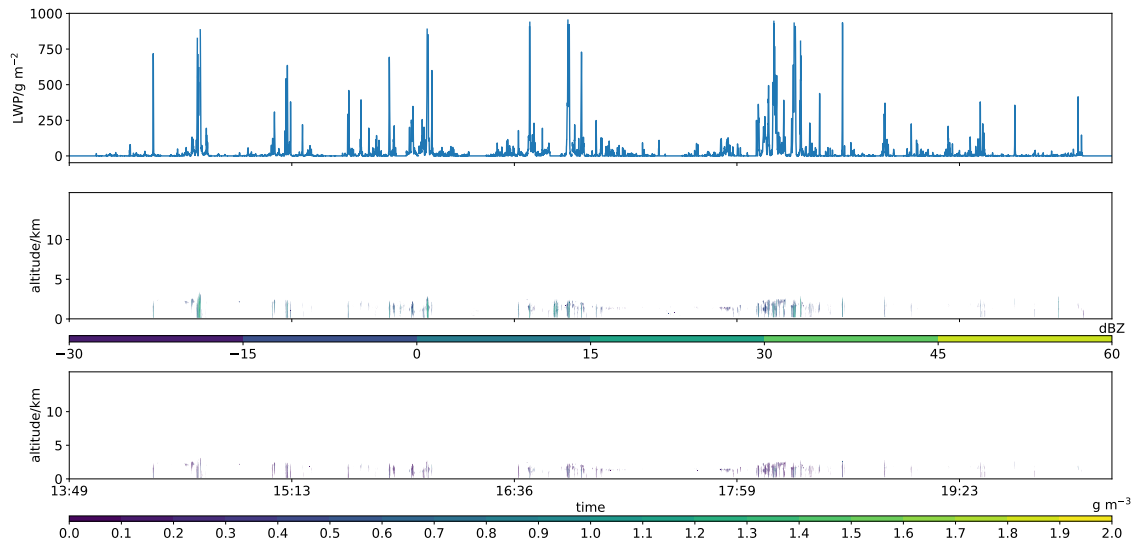


Figure 6: LWP time series in g m^{-2} (first row), profile of the equivalent reflectivity factor in dBZ with a separate color bar (second row) and calculated LWC distribution in g m^{-3} with a separate color bar (third row) for December 12, 2013. All x-axes cover the same time period.

from 0.0 (excluded) until 0.1 g m^{-3} has the strongest decrease compared to the other two flights. In contrast to the analysis of the cloud distribution, the analysis of the LWC and the range of the Z values indicates very dry and non-precipitating clouds. However, the number of values with LWC between 0.0 (excluded) and 0.2 g m^{-3} is more than twice as high as from $0.2\text{--}0.4 \text{ g m}^{-3}$ for all flights.

4.2 Discussion

All clouds during the eight analysed flights have a moist center and dryer edges. Because of entrainment of dry ambient air some cloud water evaporates to saturate the dryer air and thus reduces the LWC. In this way, the edges get even dryer than the moist regions inside the cloud. This result must be kept in mind for the following analysis. Averaging the LWC over a cloud or a cloud column does not resolve the entrainment, but gives one mean including the effects of the inner parts and the edges of the cloud.

In addition, the flights have nearly the same frequency-Z distribution and a hyperbolic frequency-LWC distribution. Low LWC values are exponentially more represented than high values during the flights. This corresponds well to the data obtained by Oh et al. (2018) analysing all existing types of clouds at the southern coast of the Republic of Korea at 34.76°N in 2014. Interpreting the Z and LWC distributions gives a better idea of the weather situation during the analysed days. On December 12, 2013 larger LWC values are more frequent compared to the other days and there are the most cases with enhanced Z values (40 dBZ). According to the Z- and LWC-frequency distributions by

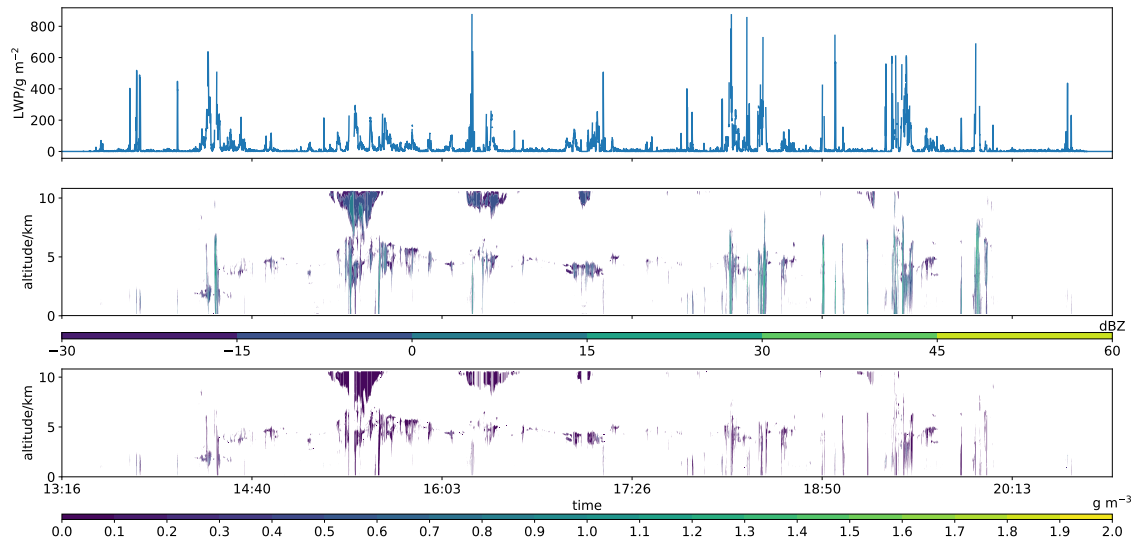


Figure 7: LWP time series in g m^{-2} (first row), profile of the equivalent reflectivity factor in dBZ with a separate color bar (second row) and calculated LWC distribution in g m^{-3} with a separate color bar (third row) for August 22, 2016. All x-axes cover the same time period.

Oh et al. (2018), this leads to the result, that more precipitating clouds exist on December 12, 2013 than on December 11, 2013 and August 22, 2016, where non-precipitating clouds predominate. This result is not indicated by the CR, because a lot of rain events and precipitating clouds are observed by the CR but neglected in the analysis by the LWP flag due to deep convection on December 11, 2013 and August 22, 2016.

In the following, the cloud types during the several flights are discussed. Marine shallow cumulus clouds are typical for the trade wind regions. Usually, this cloud type is the only cloud layer in Barbados during dry season according to Medeiros and Nuijens (2016). Generally, the clouds are located between the surface and about 3 km, the altitude of the trade wind inversion, with a cloud fraction of up to 18%. In Fig. 6 the maximum cloud amount is 6%, only one third of the maximum cloud fraction from literature. In dry season, a separated thin upper cloud layer around 10 km with a cloud fraction of 2% may exist (Medeiros and Nuijens, 2016). It is produced by the northward flowing air from the equator. The cloud fraction of the upper layer in Fig. 3 is twice as high and located around 2 km above the layer in literature, the lower layer has only 7% cloud amount, not 18% as in literature. The observation of the second cloud layer at the end of the measurement duration was near the ITCZ, because there an upper cloud layer is more likely. The lower cloud fraction of the lower layer in dry season compared to literature can be due to fewer CCN at this altitudes. The formation of this CCN distribution is explained in the following. One important process is the forming of aerosol particles during a homogeneous-bimolecular nucleation, because the outflow of a cloud is a favorable location for this nucleation. There, the molecules of two gases form one aerosol by homogeneous nucleation. The lifted air at the equator detrains at the top of the cloud with

a very low aerosol concentration due to precipitation. The air has a high RH , because of evaporating of cloud droplets due to unsaturated ambient air, and is cool, which are good conditions for a production of new aerosol particles by homogeneous-bimolecular nucleation. These new particles grow and subside. Below the inversion, they are efficient CCN even at low supersaturation (Wallace and Hobbs, 2006). The doubled cloud fraction of the upper layer on December 11, 2013 compared to literature shows that there is a higher number of droplets, thus less evaporation of cloud droplets and hence a lower RH compared to literature. However, a fundamental condition for the CCN production is a high RH . Thus, this leads to a reduced production of CCN.

In wet season, however, the ITCZ can influence the cloud cover. Due to the circulation, the ITCZ moves towards Barbados (see Sec. 1). There is a high chance of a connection of the two layers and deep convective clouds without an inversion form. The cloud fraction of the upper layer at around 13 km is up to 14%, whereas it decreases to 10% in the lower layer, which is at the same height as the lower layer in dry season (Medeiros and Nuijens, 2016). The location of the lower layer in Fig. 7 is about 1 km higher than in literature, the cloud fraction coincides with literature. The cloud fraction of the upper layer at around 9 km conforms with the fraction at 9.0 km in literature. One can see the connection of the two layers. However, it can not be said whether the cloud fraction distribution with altitude would continue like in literature because no measurements were taken at these altitudes. The observed situation is accurately described by Medeiros and Nuijens (2016). Nevertheless, it is not that easy to separate the clouds into two layers, because additional, rarely visible layers exist. Due to the missing inversion nearby the ITCZ, no lower, capped cloud layer exists. That is why only some clouds form around 2 km and why further cloud layers exist around 4 km and 9 km. There are still altitudes with higher cloud fractions but the cloud cover is continuous through the whole troposphere.

The plausibility of the observed data can be tested by comparing the measured height of the cloud bases with literature. Profiles of cloud fraction are evenly distributed between the LCL and the tops of the deepest cumuli below the trade wind inversion according to Nuijens et al. (2015). Cloudiness at the LCL dominates with two-thirds of the total cloud cover, whereas the cloudiness near cloud tops contribute another third. Cloudiness near the LCL is relatively invariant averaged over a few days, whereas cloudiness further aloft is more variant on time scales from a day to a week (Nuijens et al., 2015). In this study, most signals of Z originate at the surface. However, at the LCL, which is at a few hundred meters, no clear increase in cloud base frequency exists. The signals starting at the surface are no clouds, signals below the LCL contribute to rain. Thus, these signals are not included in the analysis by Nuijens et al. (2015). The data of this study show less cloudiness at the LCL, but a greater cloudiness at the inversion. The invariance of the cloudiness at the LCL compared to the cloud cover aloft can be seen in this data, too. The cloud cover at the LCL is changing around two percentage points during one campaign, at the inversion up to nine.

5 Dependency of LWC on altitude

As already mentioned in Sec. 4.1, there seems to be a height dependency of the LWC. Hence, the relation between altitude and LWC is investigated in this section, to derive a general LWC distribution. Cloud and rain LWC are analysed at once, even if an overlap of rain and cloud in some heights with time will give no separated trend of cloud/rain LWC. Also, the cloud height and LWC of the profiles for every time step are not normalised. Therefore, the interaction of several separated profiles of LWC with time is shown.

5.1 Results

For the analysis of the dependency of LWC on altitude, every LWC greater than 0.0 g m^{-3} at each time step is plotted against its altitude (Fig. 8). All three plots represent the cloud distribution of each case already discussed in Sec. 4. The maximum of cases for a height is always at low LWC values of $0.0\text{--}0.1 \text{ g m}^{-3}$, except for December 12, 2013 at around 1.1 km height, where the maximum is at $0.1\text{--}0.2 \text{ g m}^{-3}$. These maxima at low LWC values conform to the hyperbolically decrease of the frequency-LWC distribution shown in Sec. 4. The distribution of cases inside the first bin indicate the common cloud profile for each flight already discussed in Sec. 4. Nevertheless, the altitude of the global maximum of cases varies with every flight as well as the amount of additional maxima. There are always scattered values of high LWC, mostly in low altitudes. On December 11, 2013 (Fig. 8a) the scattered values are below 3.0 km with LWC greater than 3.0 g m^{-3} , on December 12, 2013 (Fig. 8b) and August 22, 2016 (Fig. 8c) the values are below 2.0 km with a LWC of greater than 3.6 g m^{-3} and 2.0 g m^{-3} , respectively. Thus, the great LWC values are located below the trade wind inversion.

All flights in the category represented by December 11, 2013 show two main altitudes with a maximum in cases as shown in Fig. 8a. This is due to the two layers of shallow cumuli formed during these days, one in the lower, the other one in the upper troposphere. From the additional flights analysed but not shown here in detail, only August 15, 2016 has four regions in the atmosphere with an increased number of values. However, the trend of both, the red and black line, is even there described by Fig. 8a. Because the LWC values of the extra layers are low and thus do not contribute to a higher mean value. The first maximum of cases on December 11, 2013 is at 2.0 km. The cases are increasing from the surface and decreasing abruptly just above 2.3 km, where the trade wind inversion is. Most of these cases have a LWC of $0.0\text{--}0.4 \text{ g m}^{-3}$, which tends to be high LWC values. The second maximum of cases is around 12 km. There, the cases are mostly distributed between 0.0 and 0.1 g m^{-3} . This leads to a lower average for the LWC of clouds at 12.0 km than at 2.0 km (red line). This result verifies the finding in Sec. 4. The average LWC in the upper layer is lower due to the lower Z of ice compared to liquid water, which is

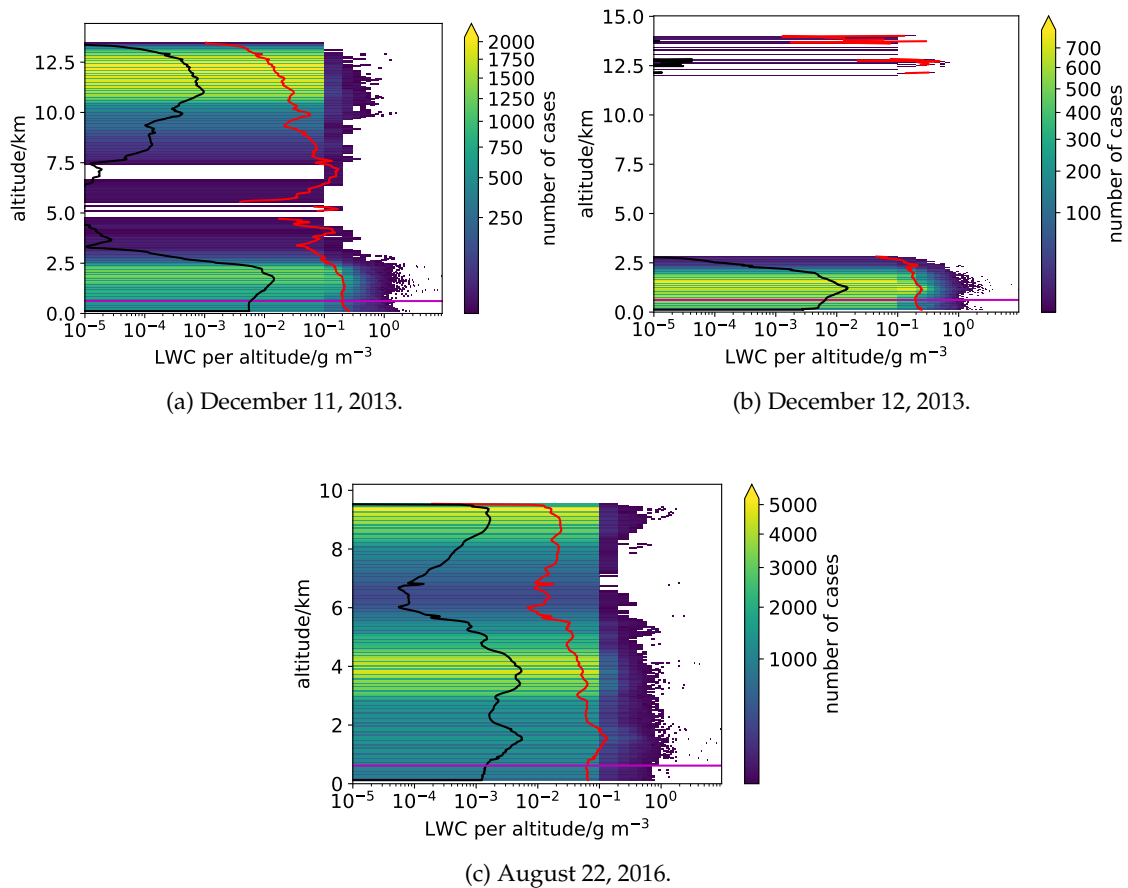


Figure 8: LWC greater than 0.0 g m^{-3} with altitude for three different flights. Average of LWC per altitude for values greater than 0.0 g m^{-3} (red line) and for all LWC values (black line). The x-axis shows the LWC per altitude in g m^{-3} , the y-axis the altitude in km. The scale of the x-axis and of the coloring, indicating the number of cases, is logarithmic. The height of LCL is marked by a magenta line.

distributed in the lower layer. Between these maxima of cases nearly no further cases are distributed. The mean values of the cloud LWC (red line) vary from 0.01 to 0.2 g m^{-3} . However, the relatively high LWC mean values of 0.2 g m^{-3} are not representative for their heights. Because at these altitudes fewer cases exist, which then can influence the development of the red line more sufficient. This is also indicated by the black line with values around 0.0 g m^{-3} . The average over all LWC values (black line), which represents the whole atmosphere, is maximal around 11 km and 2 km with 0.02 g m^{-3} . This is a very low LWC value for clouds, but not for an average over the whole measurement area with also cloudless areas.

The development of the averaged LWC over values greater than 0.0 g m^{-3} (red line) inside the first two kilometers is analysed in detail, because these values are due to the shallow cumulus clouds, which are closely investigated in this study. The averaged LWC over values greater than 0.0 g m^{-3} decreases from around 0.3 to 0.2 g m^{-3} up to the LCL,

then it is nearly constant. It then increases at around 1.5 km and is, with a LWC slightly above 0.2 g m^{-3} , constant up to around 2 km with an abrupt decrease above. This shows that the LWC distribution inside a shallow cumulus cloud is not constant with height. The reasons for this LWC distribution are discussed in Sec. 5.2.

On December 12, 2013 (Fig. 8b) the situation is similar to December 11, 2013 but with only one low cloud layer and a few, not representative values at around 13 km. There, the mean over the LWC of the clouds (red line) is relatively high with values around 0.1 g m^{-3} . However, averaged over all values it is very low (black line). Another difference is inside the distribution of the mean rain/cloud LWC in the first two kilometers (red line). The clouds have a linear increase of LWC up to 0.3 g m^{-3} at 1.0 km, followed by a slow decrease and a second maximum at 2.5 km.

The profile of August 22, 2016 (Fig. 8c) is special compared to the other flights. On the days before, higher LWC values were at the same altitude as one of the maxima of cases at very low LWC values. On August 22, 2016, this is also valid for the maxima of cases at around 4 km and 9 km. Additionally, there is a layer just below 2 km that - unlike most other layers mentioned - consists of comparatively few cases, but includes a number of high LWC values. This means that, while there are relatively few clouds in this altitude on August 22, 2016, many of them have a high LWC. The mean LWC of values greater than 0.0 g m^{-3} (red line) is lower all over the troposphere compared to the other flights. It never reaches 0.2 g m^{-3} and is constant around 0.03 with a small enhancement up to just below 0.2 g m^{-3} at 1.7 km, which decreases again up to 2.3 km. At around 6 km, a small and abrupt decrease in mean LWC can be observed. There, most clouds, which have their cloud bases slightly above the surface, have their cloud tops. The mean over all LWC values (black line) is more moderate compared to the other flights, because the humidity is not capped by a trade wind inversion and distributes over the whole troposphere. It never reaches 0.01 g m^{-3} and at the same time never falls below 0.00005 g m^{-3} .

5.2 Discussion

For this discussion a separation of the flights into cases influenced by inversion (Fig. 8a and Fig. 8b) or ITCZ (Fig. 8c) is helpful. An inversion is a barrier for air exchange, including the exchange of meteorological parameters like humidity, between the layer below the inversion and the altitudes above the inversion. Thus, the humidity is accumulated between the surface and the inversion barrier, i.e. typically 3 km in case of the trade wind inversion. That is the reason for the increase of LWC in the first kilometers during the two flights measuring an inversion. Another reason is an increased amount of CCN at this altitude due to the CCN production described in Sec. 4.2, at which droplets can form during a heterogeneous nucleation. Also, salt particles are brought into the troposphere by sea spray and capped by the inversion. Thus, clouds below the inversion have larger CCN and hence larger droplets than those above. This produces the scattered

values with a high mean LWC.

The inversion as a barrier for exchange is missing on August 22, 2016 measurement. The humidity is distributed over the whole troposphere, which leads to lower but more constant mean values of all LWC and cloud/rain LWC. The relatively high mean values over all LWC (black) say that the fraction of the cloud LWC is higher than in the other cases. This emphasises the high cloud fraction inside the ITCZ. However, also without an inversion the mean LWC decreases slightly with altitude above 2 km height. This is due to dry intrusion being maximal at the top of the clouds and spreading down the cloud. The process of dry intrusion is explained in Sec. 4.2. According to Wallace and Hobbs (2006) and Stommel (1947), air mostly entrains at the top of the cloud and while cloud water evaporates and the LWC gets reduced, the air is cooled, sinks and mixes with lower cloudy air masses.

The lower values of LWC in the upper layer on December 11, 2013 are because of a lower concentration of CCN. The additional dry intrusion at the top of a cloud increases the LWC gradient with height (Wallace and Hobbs, 2006). Another aspect is that the hydrometeors in this altitude are often ice particles. Ice has a lower radar reflectivity and thus a lower LWC. At the same time, the measurements taken are not that precise for ice compared to rain. Thus, larger errors in LWC of the upper layer are to be expected.

The trend of the averaged cloud/rain LWC would lead to the hypothesis that rain has lower LWC than the clouds, which is tested in detail in Sec. 7. The near surface increase of LWC inside the rain layer could be due to ground cluttering, which can still be notable, even after trying to reduce the effect by deleting near surface signals. This effect is missing on August 22, 2016. Here, the heavy rain characteristic for the deep convective clouds is not taken into account due to the LWP mask. Thus, less rain events than originally observed are analysed. The remaining rain events have really low LWC values. These signals are often the dry edges of a rain bulk which leads to low LWC averages. Instead there is a small enhancement in averaged LWC at around 2 km. The sun warms the air parcels, which are then lifted. The temperature of the parcels is cooled dry adiabatically. The parcels rise until they have the same temperature as the surrounding air. The amount of water vapour inside the parcels remains constant. If a parcel's dew point is greater than its temperature, a cloud will form because the water vapour will condensate on CCN. On August 22, 2016 the cloud formed at around 2 km.

The LWC distribution inside stratiform clouds is discussed in Korolev et al. (2007). The distribution is formed by adiabatic lifting and depends on cloud depth. Thus, the theory can be adopted for cumulus clouds as well. The LWC with altitude can increase, decrease or can have several maxima inside a cloud. Adiabatic lifting of air increases the LWC with altitude. The adiabatic LWC is a function of height above cloud base. In reality, the LWC is lower than the adiabatic LWC due to precipitation, radiative cooling or heating and dry intrusion (Wallace and Hobbs, 2006). The LWC of thin clouds up to 500 m thickness decreases nearly linearly up to 80% of cloud depth and decreases rapidly above. Thicker

clouds show a linear decrease of LWC up until 40% of their cloud depth, followed by a period of constant LWC and a decrease of LWC above 90% of their depth (Korolev et al., 2007).

The linear decrease can not be seen in Fig. 8 (red line). Rain below the clouds can also be found above the LCL, because the separation of rain and cloud by the LCL is not totally precise. Thus, rain LWC affect the linear decrease of the mean cloud LWC above the LCL. In Fig. 8a the constant LWC period can be seen clearly. The several maxima on December 12, 2013 could be related to the fact that a multi-cellular circulation evolved inside clouds with a separated LWC distribution in every single cell of a few hundred meter depth. The cellular circulation is enhanced by radiation. The cloud tops are cooled by emitting long wave radiation, whereas the bases are warmed by long wave radiation from the surface. Thus, the cold air masses are sinking and evaporating, while the warm air parcels are raising and growing as discussed in Korolev et al. (2007) and Wallace and Hobbs (2006). However, also the averaging over clouds having their bases at different heights could lead to several maxima.

In conclusion, it can be said that the LWC distribution with altitude depends on the stratification. During an inversion, high LWC values are found in the layer below the inversion. However, an upper cloud layer has low LWC values due to ice and dry intrusion. During a standard stratification, the humidity is distributed over the whole troposphere which leads to lower and more constant values in LWC. The linear decrease of LWC with height inside a thin cloud can not be seen in this data because of rain. Therefore, every cloud has to be analysed separately and normalised to compare the clouds. However, clouds thicker than 500 m have constant LWC values in their intermediate regions just as mentioned in literature.

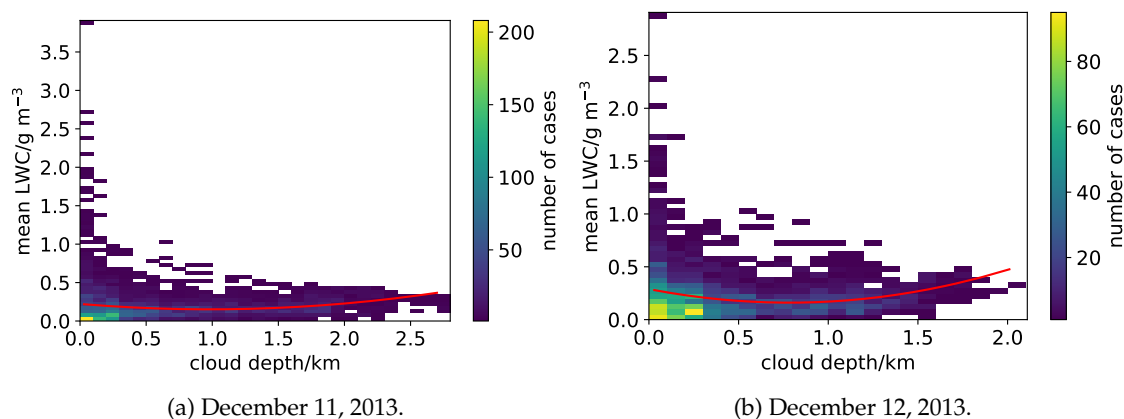


Figure 9: Frequency distribution of mean LWC in g m^{-3} over a cloud column against cloud depth in km for several flights. Only LWC values greater 0.00 g m^{-3} are shown. Regression is indicated in red.

6 LWC dependency on cloud depth

In this section, the depth of a cloud column is compared to the mean LWC of the cloud column, to find a correlation between LWC and cloud depth. Only shallow cumulus clouds are analysed in this section. Thus, cloud LWC values above the LCL, which were greater than 0.00 g m^{-3} and distributed up to 3.0 km, are taken into account. Because of the investigation of shallow cumulus clouds August 22, 2016 is not shown in the following.

6.1 Results

A correlation between cloud depth and LWC is investigated by averaging the LWC over a cloud column and compare it with the depth of the column. The patterns of the correlations seem to be parabolic for all analysed flights. In this section, the distributions are shown for December 11 and December 12, 2013 (Fig. 9). As a regression, a second-degree polynomial applies to the data points (red line). A general parametrisation of the LWC with increasing cloud depth can be done by a polynomial of second degree.

The structure of both distributions is the same: the mean values of LWC of thin cloud columns have a greater spread than those of deep columns. Deep cloud columns, however, have only moderate LWC averages. The extremely high LWC averages up to 3.95 g m^{-3} on December 11, 2013 and 2.95 g m^{-3} on December 12, 2013 are due to clouds with a depth of 0.0–0.1 km. 0.1–0.2 km deep clouds have an average up to 1.85 g m^{-3} and 1.75 g m^{-3} , respectively. Clouds deeper than 0.3 km have a mean LWC lower than 1.00 g m^{-3} , besides at 0.6 km and 0.5 km, respectively, with an average of 1.10 g m^{-3} each. The next section of the distribution is up to a depth of 1.0 km on December 11 and 1.3 km

on December 12, 2013, respectively, with an average up to 0.75 g m^{-3} . Deeper clouds have a hyperbolic decrease in the maximum of mean LWC. Very eye-catching is the additional logarithmic constraint for the minima of the average of LWC for clouds deeper than 1.8 km and 1.3 km. This constraint is also indicated by the parabolic regression. The result of the regression is, that 50 m thin clouds have a LWC around $0.20\text{--}0.30 \text{ g m}^{-3}$, clouds of 1.0 km and 0.8 km depth, respectively, have a minimal LWC of 0.15 g m^{-3} . The LWC of deeper clouds is rising up to 0.28 g m^{-3} and 0.48 g m^{-3} , respectively, for 2.0 km deep clouds. The regression is accurate for clouds deeper than 0.5 km. The LWC for thinner clouds is overestimated by the regression most times.

In conclusion, the distribution up to a cloud depth of 1.0 km is very similar for both days. For deeper clouds the development is logarithmic with nearly the same start and end mean value of LWC. Therefore, the increase is stretched over a greater cloud depth spectrum on December 11, 2013. The frequency maxima for every depth have a logarithmic distribution starting at the origin and ending in the thin domain of the LWC averages of the deepest analysed clouds.

6.2 Discussion

The discussion first concentrates on the distribution of the maxima and minima LWC averages per cloud depth (Fig. 9). Secondly, the distribution of the maximal cases is analysed. Thin clouds have both high and low averages of LWC, whereas deep clouds have only moderate mean values of LWC. High values of LWC generated by large CCN like sea salt (see Sec. 1) or erroneous high values of LWC, produced for example by insects or inaccurate measurement instruments, could lead to extreme mean values of LWC for thin clouds. The spread of values is far smaller for deep clouds, because higher numbers of values reduce the error after taking the average. This averaging effect also results in lower maxima of averaged LWC for clouds with a depth of around 0.2–1.5 km compared to thinner clouds. Furthermore, deep clouds have nearly no mean LWC values higher than 0.20 g m^{-3} . Another reason for the differences in the spread of averaged LWC could be the dry intrusion at the top of the clouds (see Sec. 5.2). If the established convection extends over the whole cloud, then there exist columns consisting of only a updraft or a downdraft. Inside a downdraft, the water is evaporating, thus the LWC is reduced. Inside a updraft, the water droplets are growing and increasing the LWC. Hence, cloud columns with very high or low averages of LWC exist. A convection through only a part of the cloud changes only a fraction of the LWC data and results in a less extreme average of LWC as it can be observed for deep clouds.

The main difference between the LWC of the regression and the distribution of the maximal cases per cloud depth is observed for thin clouds. Due to the increased spread of LWC for thin clouds the LWC of the regression is greater compared to the LWC of the maximal cases. Fewer outliers of high LWC values with increasing depth lead to a

smaller difference between the LWC values.

Korolev et al. (2007) describes the LWC distribution inside a cloud regarding the maximum of LWC inside the cloud. The result of that study is that clouds with a depth greater than 500 m have a LWC averaged over the cloud depth of around 0.14 g m^{-3} . This averaged LWC is independent of cloud depth. However, thin clouds with a depth of less than 500 m have an cloud depth dependent average of LWC, \overline{LWC} , in g m^{-3} :

$$\overline{LWC} = 0.001 \text{ g m}^{-3} \text{ m}^{-1} \cdot \Delta Z \quad (4)$$

with ΔZ being the cloud depth in meter. Water condensates inside an adiabatic lifted cloud parcel and increases its LWC for 0.001 g m^{-3} per meter for the first 500 meter. Dry intrusion at cloud top decreases the LWC of the cloud at every altitude due to convection (see Sec. 5.2). Thus, the linear increase of LWC in the first 500 m is reduced, which gets particularly notable for clouds deeper than 500 m. It is described by a linear increase of LWC over only 40% of the cloud depth and a constant trend above. There seems to be no increase of LWC by adiabatic lifting anymore. This would mean that most values of the distribution (Fig. 9) would first follow a linear function starting at 0.00 g m^{-3} , exceeding the 0.14 g m^{-3} at around 140 m cloud depth and growing up to 0.50 g m^{-3} . Then, a trend of constant LWC with 0.14 g m^{-3} averages would follow for all clouds deeper than 0.5 km. In this study, the general trend described by Korolev et al. (2007) can be found. Having a look at the bins with the highest amount of cases for each cloud depth leads to a logarithmic trend of the values. However, the distribution can not be separated into two main trends, but into three.

On December 11, 2013 (Fig. 9a) the mean LWC trend of the highest number of cases is nearly linear up to a depth of 400 m. The mean LWC reaches $0.10\text{--}0.15 \text{ g m}^{-3}$. However, the increase of LWC per meter is only around 38% of the growing rate from literature. Then, a period of cloud depth with LWC stagnating somewhere between 0.10 and 0.20 g m^{-3} follows. This is similar to literature with an constant value of 0.14 g m^{-3} . At a cloud depth of 1.9 km, the third segment begins with an increase of LWC up to around $0.30\text{--}0.35 \text{ g m}^{-3}$. This result is a contradiction to Korolev et al. (2007), who analysed a decrease for this cloud depth to 0.12 g m^{-3} . The convection may not penetrate through the whole deep cloud column and thus not affect the lower cloud layers, which lead to moderate averages.

On December 12, 2013 (Fig. 9b), the trend is a little bit different. The distribution is again starting with an increase in mean LWC, this time up to 600 m depth, one third of the depth higher than on December 11, 2013. The LWC is increasing up to $0.20\text{--}0.25 \text{ g m}^{-3}$ with a rate of 0.0004 g m^{-3} . The growing is 12% faster than on December 11, 2013. Then, the LWC is slightly decreasing again to values ranging from 0.05 until 0.20 g m^{-3} with most values between 0.10 and 0.20 g m^{-3} . The overshooting of the LWC and the constant phase coincide with literature, even if the overshooting is only half of the value from literature. For clouds deeper than 1.4 km the average of LWC is increasing up to 0.30 g m^{-3} .

In conclusion, it can be mentioned that the dry intrusion has an affect on clouds up to a depth of 500 m. The growing rate of LWC is around $0.0004 \text{ g m}^{-3} \text{ m}^{-1}$, thus lower than the adiabatic one of $0.001 \text{ g m}^{-3} \text{ m}^{-1}$. The effect of the intrusion for deeper clouds is well described by Korolev et al. (2007). For clouds deeper than around 1.7 km, however, the effect of dry intrusion is reduced again and leads to LWC averages twice that high than of slightly thinner clouds.

7 Difference in LWC of rain, precipitating and non-precipitating clouds

In the following, the mean LWC for clouds and rain is analysed, to find out whether rain has lower LWC values than clouds, as observed in Sec. 5, and whether there is a difference in the LWC for precipitating and non-precipitating clouds. Additionally, the change of the LWC of clouds and rain with the season is investigated. After applying the cloud mask mentioned in Sec. 2.3 on the calculated LWC values and separating the LWC values greater 0.00 g m^{-3} into cloud and rain LWC, the mean of the LWC is calculated for rain and clouds. Next, the clouds are separated into precipitating and non-precipitating clouds by investigating, whether the CR observed signals at the gate directly below the LCL. Then, the average of the LWC is taken for each of the two cloud categories. Just data below 2.0 km altitude are analysed, to take only shallow cumuli into account as discussed in Sec. 1.

7.1 Results

For a comparison of the LWC mean values of precipitating clouds, non-precipitating clouds and rain, the plausibility of these mean LWC values is tested first. All calculated averages of LWC are between 0.05 and 0.40 g m^{-3} (Fig. 10). These are expected values, they are characteristic for fog (Hess et al., 1998) and tradewind cumuli (Squires, 1958), respectively.

Next, seasonal differences in LWC within one category are investigated. The spread of the mean values during the flights in dry season is smaller than in wet season. The four categories of averages have a similar order for the flights during wet season apart from the mean of rain. The order of the cloud means is as follows: non-precipitating clouds have the highest LWC value, clouds in general and precipitating clouds have the lowest value. The values of non-precipitating clouds are noticeably high. August 22, 2016 is eye-catching because of generally lower mean values. This order of mean LWC implies, that the amount of droplets inside the non-precipitating clouds has to be greater or the droplets have to be bigger than inside precipitating clouds. In dry season, the order of the LWC averages is different. Precipitating clouds have the highest average, followed by clouds in general and non-precipitating clouds. In this case, the amount of droplets or size has to be greater for precipitating clouds. Only the values of December 12, 2013 follow the order of the wet season events. The averages during December 15, 2013 are nearly the same for all categories. Thus, the water content of precipitating and non-precipitating clouds is the same.

Comparing the LWC of clouds and rain shows, that clouds have greater averages of LWC than rain. That means, that clouds have a denser water content inside a unit volume than

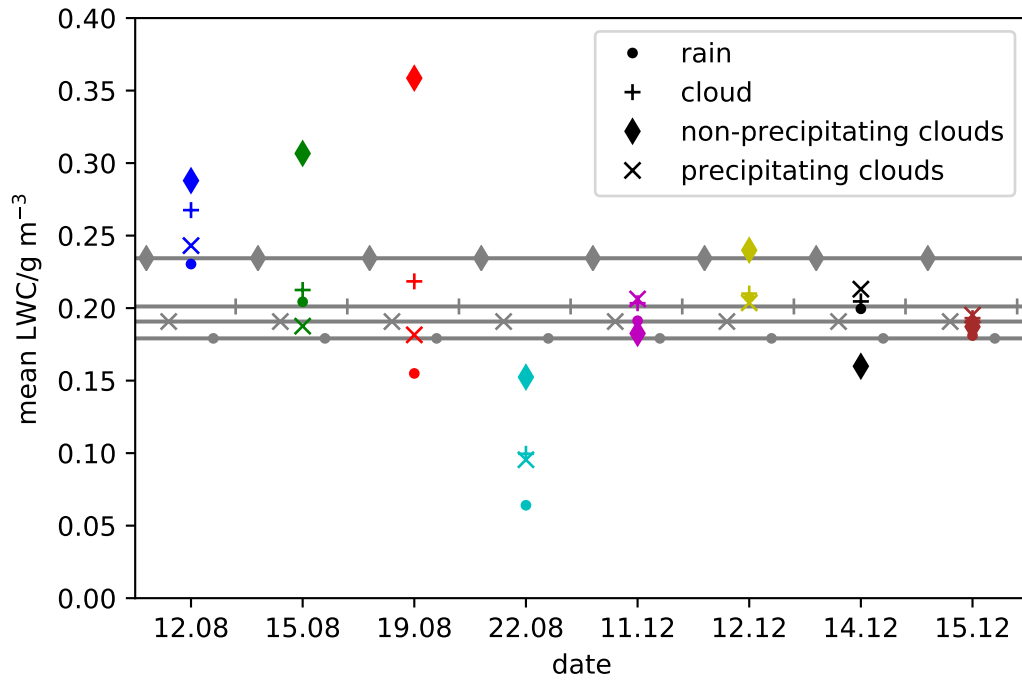


Figure 10: Mean LWC over all values greater 0.00 g m^{-3} for precipitating clouds (x), non-precipitating clouds (◆), clouds in general (+) and rain (•) for eight flights. Each day is listed on the x-axis and is indicated by its own color. The category clouds includes both precipitating and non-precipitating clouds. Grey lines indicate the average over all flights for each category.

rain. However, the LWC of rain is mostly nearby the mean of the clouds, except for August 12, August 19 and August 22, 2016.

To parameterise the LWC for each category the mean over all LWC for each category is calculated. Non-precipitating clouds have the highest average with 0.23 g m^{-3} while rain has the lowest average with 0.18 g m^{-3} . Precipitating clouds have a mean of 0.19 g m^{-3} , clouds in general of 0.20 g m^{-3} .

7.2 Discussion

First, the analysis compares the averages of the LWC values over all flights with literature. Oh et al. (2018) found out that raindrops have the highest LWC mean, followed by precipitating clouds, whereas non-precipitating clouds have the lowest mean value of LWC. In this study, the mean of the precipitating clouds is nearly the same as in literature with 0.19 g m^{-3} . Nonetheless, the mean of the precipitating clouds and rain droplets are swapped. To discuss the difference between literature and this study the wet season and dry season flights are analysed separately in the following.

The reason for lower LWC values in dry season compared to wet season is less evaporation of sea water due to less heating in dry season. Thus, the air contains less water

vapour which leads to less condensate and lower LWC values. The LWC values on August 22, 2016 are smaller across the board because of the missing inversion. The humidity is distributed over the whole troposphere, hence the LWC inside the first 2 km, where the trade wind cumulus clouds evolve, is less than in the other cases. The rain has the lowest value on August 22, 2016 because the deep convective rain events are not taken into account and the LWC of the remaining rain events is below average. This was also shown in Fig. 8c.

The LWC of rain is a little bit lower than the LWC of the clouds in average. However, on August 12 and August 22, 2016 the LWC of rain is noticeably lower than the LWC of the clouds because the increase of LWC just above the surface is missing (see Sec. 5). The LWC is getting larger with increased LWP or Z . Z is larger for an increased amount of droplets and bigger droplets. For example drizzle, which seems to be similar to clouds, has a Z of 0 dBZ and a few raindrops of 10 dBZ. The LWP will be higher, if clouds exist in lower layers. This would lead to the result, that rain has higher LWC values than clouds. In this study, the analysis is restricted to the first 2.0 km, the inversion altitude, where the LWP has no noticeable changes. Secondly, cloud droplets behave not exactly like drizzle. The formation of clouds and rain (see Sec.1) explains the difference between drizzle and cloud droplets. Thus, the condensate inside a cloud gets redistributed during a rain shower. The LWP of a column is still constant. The water of the rain originates inside the cloud and can not have a greater amount of LWC.

In the following, the LWC of the precipitating and non-precipitating clouds is analysed, which is the same as in Oh et al. (2018) for dry season, but different in wet season. In this study, the LWC of the precipitating clouds is nearly constant over the two seasons. However, the non-precipitating clouds have higher LWC values during wet season than during dry season. As described in Sec. 1, the cloud droplets of the non-precipitating clouds have a size of around $20\ \mu\text{m}$. Inside the precipitating clouds, a growing of the droplets through collection already happened and is still ongoing. Thus, also larger droplets exist inside precipitating clouds, which result in a greater Z and LWC than for non-precipitating clouds for dry season in this study. For the analysed data the situation changes during wet season and the non-precipitating clouds have higher LWC than in dry season. The LWC is dependent on Z which is in return dependent on the amount and size of droplets. The size is constant over both seasons. Hence, the amount of droplets has to be greater in wet season. In dry season, the RH is reduced and less cloud droplets get activated. A warm air parcel has a higher moisture content than a cold parcel according to the saturation vapor pressure curve. The activated cloud droplets absorb the humidity which leads to a RH higher than 100%. The humidity is again smaller at low temperatures (Wallace and Hobbs, 2006). The amount of cloud droplets and the amount of condensate is lower during dry season. After growing through condensation, the cloud droplets all have the same size but there are fewer of them during dry season than during wet season. This leads to a lower Z and LWC of non-precipitating clouds in

dry season than in wet season, as observed in this study.

However, this analysis might be inaccurate because of several reasons: First, the separation into rain and cloud is not very precise. The calculation of the height of the LCL is a simplification. In addition, it might not be representative to take the information of only a hand full sondes, to calculate the altitude of the LCL for the whole day. The altitude is interpolated for time steps over some hours. During this time the state of the atmosphere changes and so does the height of the LCL. Additionally, it is only an assumption that the LCL goes along with the base of the clouds. This is only typical for a forced lifting of air parcels. But cumulus are often formed by free convective lifting through local warming of the surface near air parcels which leads to a higher cloud base. This would count rain values as cloud values. Secondly, also cloud types other than shallow cumulus were observed. Thus, even after removing these events it affected the humidity of the remaining rain events (see August 22, 2016). Thirdly, the cloud mask does not take small clouds into account. These could change the mean values. Another point is that the LWC values have a positive bias. The CR does not observe clouds with a low number of hydrometeores, whereas the MWR is more accurate and measures low LWP. Thus, the LWP originally generated by the regions of the atmospheric column where the CR measures no Z is added to the regions with positive Z which then get a positive bias. Also, the comparison with Oh et al. (2018) is not that straight forward. They analyse clouds reaching 15 km height, not only shallow cumulus. The upper cloud layers reduce the mean LWC for clouds in that study. Furthermore, the observations of Oh et al. (2018) include a bright band. It is the melting layer of the ice particles and the beginning of the liquid rain layer. It is a region of enhanced radar reflectivity, leading to increased LWC values of rain compared to this study.

However, the section gives a rough idea, how to parameterise the LWC for precipitating and non-precipitating clouds, as well as for precipitation itself. Despite the somewhat inaccurate analysis, it can be concluded that the order of LWC averages among the different categories change with season.

8 Conclusions and outlook

In this thesis, the LWC of clouds and rain shafts over the tropical North Atlantic is calculated from LWP measurements taken by the MWR and the equivalent reflectivity factor observed by the CR. This aims at better parameterising LWC in weather models in future. In dry season, shallow cumulus clouds can be observed between the LCL and the trade wind inversion around 3 km. A second separated cloud layer at around 10 km is often visible. During wet season, the ITCZ is moving northwards and influencing the observed Barbados region. This results in the observed cloud cover extending over the whole troposphere because of the missing inversion.

For these meteorological situations, the LWC values greater than 0.0 g m^{-3} are analysed to parameterise the LWC distribution with altitude and to find differences in the distribution with changing weather situations. Due to larger CCN, higher concentrations of CCN and an accumulated humidity below the inversion compared to upper levels in the atmosphere, an average LWC of about 0.2 g m^{-3} evolves below the inversion during dry season. At the same time, fewer particles reduce the mean value of LWC at around 10 km. If no trade wind inversion exists, like during wet season, the humidity will be distributed over the whole troposphere with a light decrease of LWC with altitude because of dry intrusion.

Not only the changes of cloud LWC with altitude in the atmosphere is analysed, but also the LWC distribution with cloud depth. The maximal mean values of LWC of a cloud column decreases hyperbolically with cloud depth. However, the minima of averaged LWC are nearly 0.00 g m^{-3} to a depth of 1.5 km and increase logarithmically for deeper clouds. The spread of LWC averages is larger for thin clouds than for deeper clouds. This is due to the fact that a broader range of droplets exist in these thin clouds. E.g. dry intrusion triggers up- and downdrafts. Larger droplets originate from updrafts and smaller droplets from downdrafts. However, the up- and downdrafts have less impact on drop sizes in deeper clouds. This and additionally large CCN like sea salt lead to a wider droplet size spectrum, which is not averaged out, for thin clouds. The maximal number of cases are distributed logarithmically originating with a LWC of 0.00 g m^{-3} and ending with a LWC of around 0.30 g m^{-3} at a depth of 2.1–2.8 km. Nevertheless, the increase is linear for clouds with a depth up to 500 m. Dry intrusion has the effect that the growing rate of LWC is around $0.0004 \text{ g m}^{-3} \text{ m}^{-1}$, thus lower than the adiabatic one of $0.001 \text{ g m}^{-3} \text{ m}^{-1}$. Clouds with a depth of 0.5–1.7 km have a constant LWC average of around 0.15 g m^{-3} . The effect of the intrusion for this clouds is well described by Korolev et al. (2007). For clouds deeper than around 1.7 km, however, the effect of dry intrusion is reduced again. This leads to LWC averages of around 0.30 g m^{-3} , twice as high as the LWC of slightly thinner clouds, which was not mentioned by Korolev et al. (2007).

Because the amount of condensate from a cloud will be constant if it falls out, rain will only have the same LWC or less than the cloud. In this study, rain has lower LWC aver-

ages than clouds, with a small increase of LWC just above the surface due to ground cluttering. Precipitating clouds have a constant mean LWC of around 0.19 g m^{-3} during both seasons, whereas non-precipitating clouds have a higher LWC during wet season than during dry season. The averaged LWC for non-precipitating over all flights is 0.23 g m^{-3} . During wet season, the amount of droplets is larger than during dry season, because RH is enhanced and more cloud droplets get activated. This results in a larger Z and greater mean values of LWC for non-precipitating clouds.

As an improvement of this study, a more accurate splitting of rain and cloud LWC could be done in future. This reduces the influence of rain LWC on averages of cloud LWC and vice versa due to a wrong separation. It would be reached by a more precise calculation of the LCL, more sonde measurements to get a smaller period of interpolation for the LCL height or by combining the output of the different channels of the MWR, which can distinguish rain and clouds. For some flights, it could be helpful to analyse periods of different cloud cover separately to investigate the different cloud types severally. The measurements of December 11, 2013 for example can be split up into three periods before the investigation. The first period would be from the beginning of the flight until 19:10 h, where only one low cloud layer exists, the second one would last until 20:30 h, a period with an upper cloud layer, and the third would be until the end of the flight, a section with two cloud layers. It is also interesting to analyse the dependency of cloud LWC with altitude as already done in Korolev et al. (2007). A normalization of the profiles regarding cloud depth and maximum LWC for different intervals in cloud depth would lead to a general LWC distribution inside a cloud. This would give an idea of the cloud LWC trend in the first 500 m above the cloud base. This would be helpful to review the study of Korolev et al. (2007). Only eight flights of the NARVAL campaign were analysed because of return flights and failing measurement instruments. An analysis based on more data is necessary to generalise the results of this study. For this, measurements that will be taken during the campaign EUREC⁴A near Barbados in January until March 2019 can be used.

In future, more campaigns like EUREC⁴A are necessary to get an idea of the impact of climate change on the forming of shallow cumulus clouds and changes in their LWC due to higher temperatures in future. An investigation of the time when the mean LWC of non-precipitating clouds is changing from being higher to being lower than the mean of precipitating clouds would be interesting as well. The delay of the change regarding the solar elevation of 90° at one geographical latitude in spring and autumn would be important for modelling. At the same time, the influence of the heat capacity of the ocean on the evaporation of the water could be worth analysing.

Acknowledgements

First and foremost, I would like to thank my supervisors Dr. Heike Konow and Prof. Dr. Felix Ament for their support during my work on this thesis and for the feedback they gave me in the end. I am really grateful that they came up with such an interesting topic for my Bachelor's thesis after the first meeting. Special thanks to Dr. Heike Konow for answering all my questions.

For the LWP data I acknowledge Marek Jacob of the University of Cologne for making the data available. Additional thanks to Dr. Heike Konow for providing the HAMP data.

Both data are available at <https://cera-www.dkrz.de/WDCC/ui/cerasearch/>.

None of this could have happened without my fellow students (Alena, Annika, Flo, Jon, Milica, Moritz, Ralph, Theresa), who gave me input and cheered me up during the whole work.

List of Figures

1	Conceptual model of the vertical profile of the Hadley cell across the tropical North Atlantic (by Tes blendspace (2019), modified by Imke Schirmacher).	2
2	Flight pattern of all flights during NARVAL South (left) and NARVAL2 (right). Each campaign day is indicated by its own color. The map section is near Barbados.	4
3	LWP time series in g m^{-2} (first row), profile of the equivalent reflectivity factor in dBZ with a separate color bar (second row) and calculated LWC distribution in g m^{-3} with a separate color bar (third row) for December 11, 2013. All x-axes cover the same time period. The black lines indicate the three sections, the profile can be split into.	10
4	Histogram of (a) LWC in g m^{-3} and (b) Z in dBZ for December 11, 2013. Both y-axes show the number of cases.	11
5	LWP time series in g m^{-2} (first row), profile of the equivalent reflectivity factor in dBZ with a separate color bar (second row) and calculated LWC distribution in g m^{-3} with a separate color bar (third row) for December 11, 2013. All x-axes cover the same time period. The profile is a close-up of Fig. 3, it is beginning at 20:18 h.	12
6	LWP time series in g m^{-2} (first row), profile of the equivalent reflectivity factor in dBZ with a separate color bar (second row) and calculated LWC distribution in g m^{-3} with a separate color bar (third row) for December 12, 2013. All x-axes cover the same time period.	13
7	LWP time series in g m^{-2} (first row), profile of the equivalent reflectivity factor in dBZ with a separate color bar (second row) and calculated LWC distribution in g m^{-3} with a separate color bar (third row) for August 22, 2016. All x-axes cover the same time period.	14
8	LWC greater than 0.0 g m^{-3} with altitude for three different flights. Average of LWC per altitude for values greater than 0.0 g m^{-3} (red line) and for all LWC values (black line). The x-axis shows the LWC per altitude in g m^{-3} , the y-axis the altitude in km. The scale of the x-axis and of the coloring, indicating the number of cases, is logarithmic. The height of LCL is marked by a magenta line.	17
9	Frequency distribution of mean LWC in g m^{-3} over a cloud column against cloud depth in km for several flights. Only LWC values greater 0.00 g m^{-3} are shown. Regression is indicated in red.	21

-
- 10 Mean LWC over all values greater 0.00 g m^{-3} for precipitating clouds (x), non-precipitating clouds (\blacklozenge), clouds in general (+) and rain (\bullet) for eight flights. Each day is listed on the x-axis and is indicated by its own color. The category clouds includes both precipitating and non-precipitating clouds. Grey lines indicate the average over all flights for each category. 26

References

- Bony, S., B. Stevens, F. Ament, S. Bigorre, P. Chazette, S. Crewell, J. Delanoë, K. Emanuel, D. Farrell, C. Flamant, et al. (2017). "EUREC⁴A: A Field Campaign to Elucidate the Couplings Between Clouds, Convection and Circulation". In: *Surveys in Geophysics* 38.6, pp. 1529–1568. DOI: 10.1007/s10712-017-9428-0.
- Bremen, L. V., E. Ruprecht, and A. Macke (2002). "Errors in liquid water path retrieval arising from cloud inhomogeneities: The beam-filling effect". In: *Meteorologische Zeitschrift* 11.1, pp. 13–19. DOI: 10.1127/0941-2948/2002/0011-0013.
- Fabry, F. (2015). *Radar meteorology: Principles and Practice*. Cambridge University Press.
- Frisch, A. S., B. E. Martner, I. Djalalova, and M. R. Poellot (2000). "Comparison of radar/radiometer retrievals of stratus cloud liquid-water content profiles with in situ measurements by aircraft". In: *Journal of Geophysical Research: Atmospheres* 105.D12, pp. 15361–15364. DOI: 10.1029/2000JD900128.
- Hess, M., P. Koepke, and I. Schult (1998). "Optical Properties of Aerosols and Clouds: The Software Package OPAC". In: *Bulletin of the American meteorological society* 79.5, pp. 831–844. DOI: 10.1175/1520-0477(1998)079<0831:OPOAAC>2.0.CO;2.
- Jacob, M., F. Ament, M. Gutleben, H. Konow, M. Mech, M. Wirth, and S. Crewell (2019a). "Investigating the liquid water path over the tropical Atlantic with synergistic airborne measurements". In: *Atmospheric Measurement Techniques* 12.6, pp. 3237–3254. DOI: 10.5194/amt-12-3237-2019.
- Jacob, M., F. Ament, M. Gutleben, H. Konow, M. Mech, M. Wirth, and S. Crewell (2019b). *Liquid water path and integrated water vapor over the tropical Atlantic during NARVAL-South*. DOI: 10.26050/WDCC/HALO_measurements_5.
- Jacob, M., F. Ament, M. Gutleben, H. Konow, M. Mech, M. Wirth, and S. Crewell (2019c). *Liquid water path and integrated water vapor over the tropical Atlantic during NARVAL2*. DOI: 10.26050/WDCC/HALO_measurements_6.
- Karimian, A., C. Yardim, P. Gerstoft, W. S. Hodgkiss, and A. E. Barrios (2011). "Refractivity estimation from sea clutter: An invited review". In: *Radio Science* 46.06, pp. 1–16. DOI: 10.1029/2011RS004818.
- Klocke, D., M. Brueck, C. Hohenegger, and B. Stevens (2017). "Rediscovery of the doldrums in storm-resolving simulations over the tropical Atlantic". In: *Nature Geoscience* 10.12, pp. 891–896. DOI: 10.1038/s41561-017-0005-4.
- Konow, H. (2019). *private communication*. (2019-03-29).
- Konow, H., M. Jacob, F. Ament, S. Crewell, F. Ewald, M. Hagen, L. Hirsch, F. Jansen, M. Mech, and B. Stevens (2018a). *HALO Microwave Package measurements during Next-generation Remote sensing for VALIDation Studies - South (NARVAL-South)*. DOI: 10.1594/WDCC/HALO_measurements_2.
- Konow, H., M. Jacob, F. Ament, S. Crewell, F. Ewald, M. Hagen, L. Hirsch, F. Jansen, M. Mech, and B. Stevens (2018b). *HALO Microwave Package measurements during Next-*

- generation Remote sensing for VALidation Studies 2 (NARVAL2). DOI: 10.1594/WDC/ HALO_measurements_3.
- Korolev, A., G. Isaac, J. Strapp, S. Cober, and H. Barker (2007). "In situ measurements of liquid water content profiles in midlatitude stratiform clouds". In: *Quarterly Journal of the Royal Meteorological Society* 133.628, pp. 1693–1699. DOI: 10.1002/qj.147.
- Levin, Z. and W. R. Cotton (2008). *Aerosol Pollution Impact on Precipitation: A Scientific Review*. Springer Science & Business Media.
- Löhnert, U, S Crewell, C Simmer, and A. Macke (2001). "Profiling Cloud Liquid Water by Combining Active and Passive Microwave Measurements with Cloud Model Statistics". In: *Journal of Atmospheric and Oceanic Technology* 18.8, pp. 1354–1366. DOI: 10.1175/1520-0426(2001)018<1354:PCLWBC>2.0.CO;2.
- Mech, M., E Orlandi, S Crewell, F. Ament, L. Hirsch, M Hagen, G Peters, and B. Stevens (2014). "HAMP-the microwave package on the High Altitude and LOng range research aircraft HALO". In: *Atmospheric Measurement Techniques* 7, pp. 4539–4553.
- Medeiros, B. and L. Nuijens (2016). "Clouds at Barbados are representative of clouds across the trade wind regions in observations and climate models". In: *Proceedings of the National Academy of Sciences* 113.22, E3062–E3070. DOI: 10.1073/pnas.1521494113.
- Miyamoto, Y., Y. Kajikawa, R. Yoshida, T. Yamaura, H. Yashiro, and H. Tomita (2013). "Deep moist atmospheric convection in a subkilometer global simulation". In: *Geophysical Research Letters* 40.18, pp. 4922–4926. DOI: 10.1002/grl.50944.
- Nuijens, L., B. Medeiros, I. Sandu, and M. Ahlgrimm (2015). "The behavior of trade-wind cloudiness in observations and models: The major cloud components and their variability". In: *Journal of Advances in Modeling Earth Systems* 7.2, pp. 600–616. DOI: 10.1002/2014MS000390.
- Oh, S.-B., Y. H. Lee, J.-H. Jeong, Y.-H. Kim, and S. Joo (2018). "Estimation of the liquid water content and Z-LWC relationship using Ka-band cloud radar and a microwave radiometer". In: *Meteorological Applications* 25.3, pp. 423–434. DOI: 10.1002/met.1710.
- Riehl, H. et al. (1979). *Climate and Weather in the Tropics*. Academic Press.
- Squires, P (1958). "The Microstructure and Colloidal Stability of Warm Clouds: Part I – The Relation between Structure and Stability". In: *Tellus* 10.2, pp. 256–261.
- Stevens, B. and S. Bony (2013a). "Water in the atmosphere". In: *Phys. Today* 66.6, p. 29. DOI: 10.1063/PT.3.2009.
- Stevens, B. and S. Bony (2013b). "What Are Climate Models Missing?" In: *Science* 340.6136, pp. 1053–1054. DOI: 10.1126/science.1237554.
- Stevens, B., F. Ament, S. Bony, S. Crewell, F. Ewald, S. Gross, A. Hansen, L. Hirsch, M. Jacob, T. Kölling, et al. (2019). "A high-altitude long-range aircraft configured as a cloud observatory-the NARVAL expeditions". In: *Bulletin of the American Meteorological Society*. DOI: 10.1175/BAMS-D-18-0198.1.

- Stommel, H. (1947). "ENTRAINMENT OF AIR INTO A CUMULUS CLOUD". In: *Journal of Meteorology* 4.3, pp. 91–94. DOI: 10.1175/1520-0469(1947)004<0091:EOAIAC>2.0.CO;2.
- Tes blendspace (2019). *Trade Wind Inversion*. URL: <https://www.tes.com/lessons/JrBH5-EfoPlo6g/wind> (visited on 10/25/2019).
- Wallace, J. M. and P. V. Hobbs (2006). *Atmospheric Science: An Introductory Survey*. Elsevier.
- Watts, S., K. Ward, and M. Greco (2016). *Radar Performance in Clutter - Modelling, Simulation and Target Detection Methods*. EURAD The 13th European Radar Conference. URL: <https://intranet.birmingham.ac.uk/eps/documents/public/emuw2/WF02.pdf> (visited on 09/09/2019).

Versicherung an Eides statt

Hiermit versichere ich an Eides statt, dass ich die vorliegende Arbeit im Studiengang B.Sc. Meteorologie selbstständig verfasst und keine anderen als die angegebenen Hilfsmittel – insbesondere keine im Quellenverzeichnis nicht benannten Internet-Quellen – benutzt habe. Alle Stellen, die wörtlich oder sinngemäß aus Veröffentlichungen entnommen wurden, sind als solche kenntlich gemacht. Ich versichere weiterhin, dass ich die Arbeit vorher nicht in einem anderen Prüfungsverfahren eingereicht habe und die eingereichte schriftliche Fassung der auf dem elektronischen Speichermedium entspricht.

Ich bin mit einer Einstellung in den Bestand der Bibliothek des Fachbereiches einverstanden.

Hamburg, den _____ Unterschrift: _____